



# Processability of DDS Isomers-Cured Epoxy Resin: Effects of Amine/Epoxy Ratio, Humidity, and Out-Time

Daniel Kim\* and Steven R. Nutt

Department of Chemical Engineering and Materials Science, University of Southern California, Los Angeles, CA, 90089-0241, USA

\* E-mail: kim344@usc.edu

**Abstract:** Three aerospace grade resins were formulated to investigate the effects of variation in DDS isomers, amine-to-epoxy (a/e) stoichiometric ratio, out-time, and moisture absorption on processing characteristics and cured resin properties. Such resins are typically used in prepreg or preimpregnated composite fibers, which require engineered processing methods to fully impregnate the fiber bed during cure. Precure phenomena, specifically out-time and moisture absorption, are generally unavoidable in practice, and these phenomena were investigated to determine the relationship between DDS isomers, a/e stoichiometric ratio, out-time, and moisture absorption on processing characteristics and cured resin properties. Furthermore, predictive models were developed to provide insights into defect formation mechanisms and mitigation strategies for prepreg processing.

Key words: curing of polymers, viscosity, resins, thermosets

## INTRODUCTION

Epoxy resins are widely used as matrix materials for prepreg or preimpregnated composite fibers which in turn are used in high-performance composites applications, including primary aerospace structures. Upon curing, epoxy resins maintain the part shape, protect the fibers from environmental degradation, and transfer loads to the fibers [1–3]. Aerospace grade epoxy resins are typically

Please cite the article as: D. Kim, and S.R. Nutt, “Processability of DDS Isomers-Cured Epoxy Resin: Effects of Amine/Epoxy Ratio, Humidity, and Out-Time” Polymer Engineering and Science. 2017. DOI: 10.1002/pen.24738



composed of multifunctional epoxies, aromatic cure agents, and tougheners, such as thermoplastics or liquid rubbers. The resins are formulated to meet the desired processing characteristics (i.e., cure kinetics and viscosity [ $\eta$ ] evolution) and to yield the properties required of the cured resin, primarily glass transition temperature ( $T_g$ ) and mechanical property values. Among the variables involved in resin formulation, cure agent type and amine-to-epoxy (a/e) stoichiometric ratio have been shown to affect processing characteristics and cured resin properties the most [4–6].

Epoxy resin cured with diaminodiphenyl sulfone (DDS), an aromatic cure agent, is widely used for aerospace grade matrices [6–9]. The two isomers of DDS are 3,3'-DDS (33DDS), which features a meta-substitution, and 4,4'-DDS (44DDS), which has a para-substitution. Studies have shown that these isomers result in different resin processing and cured properties due to different energy dissipation mechanisms [6, 7]. The 33DDS-based resins generally exhibit greater flexibility than 44DDS-based resins because of higher configurational entropy. This flexibility allows the polymer chains to rearrange at lower temperatures, eliminating free volume to form more tightly packed amorphous networks (or less free volume), thereby resulting in lower  $T_g$  values than 44DDS-based resins. In addition, the a/e stoichiometric ratio has been shown to have complex effects on cured resin properties, where optimal thermal and mechanical properties are obtained at different a/e stoichiometric ratios due to phase separation within the resin [5]. Lower a/e stoichiometric ratios generally require longer dwells at higher temperature to complete etherification caused by excess epoxy groups.

The production of high quality, defect-free composite parts requires defect mitigation strategies. Especially, it is important to tailor cure cycles that yield the required resin flow into fiber beds prior to gelation, the point at which resin flow stops. During precure operations, the resin state can be affected by environmental factors such as out-time and ambient humidity [10–15]. Extended out-



time can advance the degree of cure ( $\alpha$ ) and viscosity ( $\eta$ ) of the resin, potentially preventing full infiltration of the fiber bed prior to cure. Exposure to ambient humidity during out-time leads to absorption of moisture. The absorbed moisture can then evolve during cure, causing the growth of voids. In addition, moisture absorption has also been shown to affect  $\alpha$  and  $\eta$  of the resin by acting as both catalyst and solvent for the amine-epoxy cure reaction [10–13].

There have been few studies relating the effects of variation in DDS isomers and a/e stoichiometric ratio on resulting cured properties [6–9]. However, there have been no studies reporting the effects of variation in DDS isomers, a/e stoichiometric ratio, out-time, and moisture absorption on processing characteristics. In addition, cure kinetics and g modelling accounting for these variables could offer insights into effects that could be useful to develop defect mitigation strategies (e.g., flow-enhanced cure cycle) for manufacturing composite parts.

Therefore, in this work, three resin systems were created, varying DDS isomers and a/e stoichiometric ratio, and these were subjected to several levels of out-time and humidity conditioning. The key objectives of the study were to develop:

1. A methodology for quantifying the a prior to cure of each resin systems subjected to humidity conditioning as well as out-time.
2. Models for cure kinetics and g that capture the effects of variation in DDS isomers, a/e stoichiometric ratio, out-time, and moisture absorption.

In addition, process critical parameters were analyzed, including gelation time ( $t_{gel}$ ) and minimum viscosity ( $\eta_{min}$ ), which influence resin flow time and a cured resin property,  $T_g$ .



We show that accurate process models that comprehensively capture out-time and humidity effects on cure kinetics and  $\eta$  in process conditions for all three resin systems can be developed.

Variation in DDS isomers and a/e stoichiometric show tradeoff between cure rate, resin flow time, and  $T_g$ . Furthermore, we demonstrate that accurate process models allow control of resin flow, thereby potentially mitigating flow-induced defects during prepreg processing.

## EXPERIMENTAL

### *Materials*

The epoxy resin mixture components used are shown in Fig. 1. Each of the epoxy resin mixture compositions evaluated here contained two epoxy resins and a thermoplastic polymer. The epoxy resins comprised a tetrafunctional epoxy, tetraglycidyl-4,4'-methylenebisbenzenamine (TGMDA; MY721, epoxy equivalent weight (EEW) ~112; Huntsman Advanced Materials) and a trifunctional epoxy, triglycidyl p-aminophenol (TGAP; MY0510, EEW ~101; Huntsman Advanced Materials). A widely used impact modifier, a thermoplastic toughening agent, comprised a functionalized polyether sulfone (PES; SUMIKAEXCEL PES 5003P; Sumitomo Chemical Company). The curing agents used in the resin mixtures were the aromatic amines: 4,4'-diaminodiphenyl sulfone (44DDS; Aradur 9664-1, amine hydrogen equivalent weight [AHEW] ~62; Huntsman Advanced Materials) or 3,3'-diaminodiphenyl sulfone (33DDS; Aradur 9719-1, AHEW ~62; Huntsman Advanced Materials). Weight percent (wt%) ratio between TGMDA: TGAP was fixed at 50:50, and PES comprised 15 wt% of the overall resin mixture components. Cure agent type and amine-to-epoxy (a/e) stoichiometric ratio were varied to formulate following three formulations: (1) 33DDS with a/e = 0.8; (2) 33DDS with a/e = 0.6; and



(3) 44DDS with a/e = 0.8. These formulations were chosen to yield the properties of a typical aerospace grade epoxy resin [9].

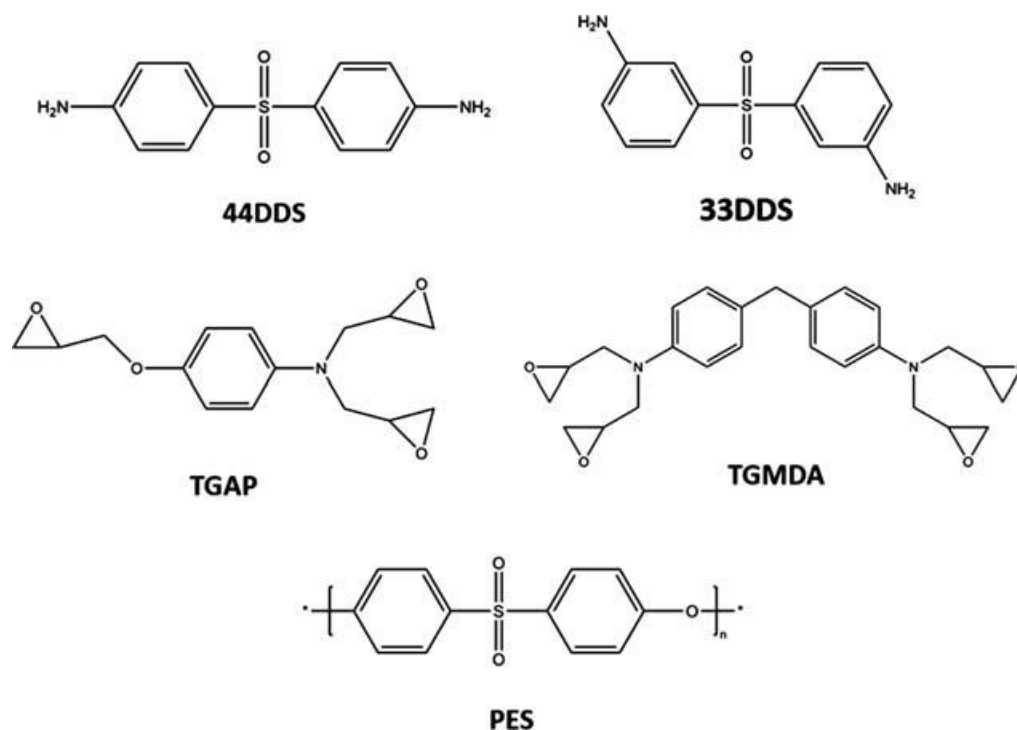


FIG. 1. Resin mixture component structures—4,4'-diaminodiphenyl sulfone (44DDS), 3,3'-diaminodiphenyl sulfone (33DDS), triglycidyl p-aminophenol (TGAP), tetraglycidyl-4,4'-methylenebisbenzenamine (TGMDA), and polyethersulphone (PES).

Each resin mixture was prepared following the same procedure. TGAP and TGMDA (50:50) were added to an aluminium container, and the container was placed into a convection oven, where mixing began. The temperature was increased to ~110°C, and PES was added and fully dissolved into the resin. Subsequently, the oven was cooled to 80°C, and the specified stoichiometric level of 33DDS or 44DDS was mixed into the resin. Mixing temperatures used herein were low enough to



have negligible effect on epoxy amine cure. Once a transparent solution was achieved, the solution was allowed to cool. The samples were then stored in a freezer below -12°C before use.

#### *Sample Conditioning: Humidity and Out-Time Control*

The initial out-time of all resin mixtures was taken to be 0 days. All samples were aged in humidity chambers containing saturated salt solutions, affording accurate control of equilibrium vapor pressure. Chambers were maintained at  $23 \pm 1^\circ\text{C}$  and at relative humidity (rh) levels of 30, 60, and 90% for 0–30 days. Subsequent testing was performed within 10 days.

#### *Modulated Dynamic Scanning Calorimetry*

Modulated dynamic scanning calorimetry (MDSC) measurements were conducted under a constant N<sub>2</sub> flow of 50 mL/min (TA Instruments Q2000). For each measurement, ~10 mg of resin was sealed in aluminum hermetic pans (Tzero, TA Instruments). Nonisothermal cures were conducted by heating the DSC cell from -60°C to 280°C at a constant heating rate of 3.0°C/min with a temperature modulation of  $\pm 0.5^\circ\text{C}/\text{min}$ . The total heat of reaction ( $\Delta H_T$ ) of the resin was determined by integrating the heat flow evolution from these measurements. Isothermal dwells were performed at 121 and 150°C for day 0 samples to build an accurate base for cure kinetics models. Isothermal dwells were also performed at 150°C for rh levels of 30, 60, and 90% for days 10, 20, and 30 to quantify the effects of moisture absorption and outtime or aging on cure. After all isothermal tests, the DSC cell was cooled to 20°C, then heated to 280°C at a constant heating rate of 3.0°C/min to measure the residual heat of reaction ( $\Delta H_R$ ). The thermal stability of the resin was determined by thermogravimetric analysis (TGA Q800, TA Instruments). Between 20°C and



280°C, the resin weight decreased by less than 0.5%, excluding the amount water absorbed by the resin, indicating that no resin degradation took place.

### *Rheometry*

Viscosity ( $\eta$ ) measurements were conducted using aluminium parallel plates in a rheometer (TA Instruments AR2000). All tests were performed under constant oscillatory shear at a frequency of 1 Hz and at strain of 0.25%, within the linear viscoelastic (LVE) regime of all resin systems. The resin samples were sandwiched between aluminum parallel plates and compressed to a gap of 0.5 mm. Nonisothermal cures were conducted by heating at 3.0°C/min to 280°C, and isothermal dwells were performed by heating at 10°C/min to 121 and 150°C for day 0 samples to build accurate base cure kinetics models, and at 150°C for rh levels of 30, 60, and 90% for day 10, 20, and 30 to quantify effects of moisture absorption and aging on viscosity evolution. For both nonisothermal and isothermal tests, the stopping condition was defined as 90% of the machine-specified maximum torque (200 mN•m) to ensure that measurements extended to and beyond the gel point as feasible.

## **THEORETICAL BACKGROUND**

### *Cure Kinetics Model*

The following steps were taken to model cure kinetics. First,  $\Delta H_T$  was determined from nonisothermal cure data by fully curing the day 0 sample. Then, assuming that a cure rate is directly proportional to the measured heat flow, the cure rate can be expressed as [16, 17]:



$$\frac{d\alpha}{dt} = \frac{1}{\Delta H_T} \frac{dH}{dt} \quad (1)$$

where  $\alpha$  is the degree of cure,  $d\alpha/dt$  is the cure rate, and  $dH/dt$  is the measured heat flow.

Integration of  $d\alpha/dt$  versus time then yields  $\alpha$  as a function of time.

Epoxy cure reactions are complex, where linear chain extension and crosslinking take place concurrently. Therefore, phenomenological cure kinetics models are generally used to model epoxy cure reactions versus mechanical models [17–19]. In this study, a phenomenological model [19] accounting for the interplay between kinetics-controlled and diffusion-controlled reactions was modified to capture the effects of out-time and moisture absorption, yielding the following form:

$$\frac{d\alpha}{dt} = \frac{K_i \alpha^{m_i} (1 - \alpha)^{n_i}}{1 + \exp^{(D_i (\alpha - (\alpha_{C0,i} + \alpha_{CT,i} T)))}} \quad (2)$$

$$K_i = A_i \exp \left[ \frac{-E_{A,i}}{RT} \right]_{i=1,2} \quad (3)$$

where  $K_i$  is the Arrhenius temperature-dependent term,  $A_i$  is the Arrhenius constant,  $E_{A,i}$  is the activation energy,  $m_i$  and  $n_i$  are reaction order-based fitting constants,  $D$  is the diffusion constant,  $T$  is the temperature,  $\alpha_{C0}$  is the critical degree of cure at absolute zero, and  $\alpha_{CT}$  accounts for the increase in critical degree of cure with temperature. The numerator from equation (2) describes an Arrhenius-type autocatalytic reaction, while the denominator adds a diffusion factor to account for the shift from a kinetics-controlled reaction to a diffusion-controlled reaction as  $\alpha$  increases. To account for ambient temperature and moisture absorption induced cure, which induce both time and magnitude shifts in the  $d\alpha/dt$  profile, the initial degree of cure ( $\alpha_0$ ) and the variables  $A_i$ ,  $m_i$ ,  $n_i$ ,





$D_i$ ,  $\alpha_{C0,i}$ , and  $\alpha_{CT,i}$  were defined as the general form  $f(r, t_o) = g(r)t_o^2 + h(r)t_o + i(r)$ , where  $g(r)$ ,  $h(r)$  and  $i(r)$  are second-order polynomials,  $r$  is relative humidity, and  $t_o$  is out-time. The model parameters determined are provided in Tables S1-S4.

TABLE S1. Parameters for cure kinetics model for 33DDS (a/e = 0.6) (where rh = rh in fraction and  $t_o$  = out-time in days)

$A_1 (x10^4 s^{-1}) = (8.90rh^2 - 10.8rh + 6.51)x10^{-2}t_o^2 + (-1.62rh + 5.17)t_o + (5.0rh + 146)$
$E_{A1}/R (x10^{-1} K) = (1.33rh^2 - 1.47rh + 59.2)x10^{-2}t_o^2 + (-6.33rh^2 + 7.37rh - 3.18)t_o + (-1.67rh - 168)$
$m_1 (x10^2) = (-22.2rh^2 + 27.6r - 2.01)x10^{-2}t_o^2 + (8.89rh^2 - 11.0rh - 11.9)x10^{-1}t_o + (9.44rh^2 - 9.83rh - 70.3)$
$n_1 (x10^2) = (-7.31rh + 1.83)x10^{-3}t_o^2 + (2.59rh - 1.01)x10^{-1}t_o + (-1.17rh^2 - 1.58rh + 8.27)$
$D_1 = (-1.07rh + 2.87)x10^{-4}t_o^2 + (4.07rh - 13.3)x10^{-3}t_o + 1.40$
$\alpha_{C0,1} = (7.08rh^2 - 8.15rh + 1.96)x10^{-1}t_o^2 + (-21.8rh^2 + 26.2rh - 6.73)t_o - 49.7$
$\alpha_{CT,1} = 1.10x10^{-2}$
$A_2 (x10^4 s^{-1}) = (28.9rh^2 - 30.9rh + 8.86)x10^{-3}t_o^2 + (-3.22rh^2 - 3.35rh - 1.84)x10^{-1}t_o + 10.6$
$E_{A2}/R (K) = -9.37x10^{-2}$
$m_2 (x10^2) = (-5.10rh - 1.54)x10^{-1}t_o + (-8.89rh^2 + 8.67rh + 76.9)$
$n_2 (x10^1) = 4.30x10^{-3}t_o^2 + (28.3rh^2 - 23.9rh + 5.68)x10^{-1}t_o + (-1.33rh + 29.1)$



$D_2 = (-19.8rh^2 + 23.7rh - 4.10) \times 10^{-2}t_o^2 + (50.1rh^2 - 58.6rh + 7.40) \times 10^{-1}t_o + (-6.67rh^2 - 8.0rh + 51.5)$
$\alpha_{C0,2} = -7.72 \times 10^{-5}$
$\alpha_{CT,2} (x10^3) = (198rh^2 - 260rh + 6.50) \times 10^{-4}t_o + 1.66$

TABLE S2. Parameters for cure kinetics model for 33DDS (a/e = 0.8)

$A_1 (x10^2s^{-1}) = (27.4rh - 1.16) \times 10^{-4}t_o^2 + (-100rh - 1.80) \times 10^{-3}t_o + (1.40)$
$E_{A1}/R (x10^{-3}K) = (4.98rh^2 - 7.69rh + 1.88) \times 10^{-3}t_o^2 + (-15.0rh^2 + 23.6rh - 5.41) \times 10^{-2}t_o - 1.44$
$m_1 (x10^1) = (6.81rh^2 - 5.71rh + 1.91) \times 10^{-3}t_o^3 + (19.6rh^2 - 20.7rh + 1.71) \times 10^{-2}t_o^2 + (16.1rh - 4.45) \times 10^{-1}t_o - 7.69$
$n_1 (x10^1) = (19.3rh^2 - 23.2rh + 6.98) \times 10^{-3}t_o^2 + (-5.46rh^2 + 6.01rh - 1.78) \times 10^{-1}t_o + (-1.33rh^2 - 1.43rh + 3.54)$
$D_1 = (28.2rh + 5.63) \times 10^{-3}t_o^2 + (-60.8rh - 4.23) \times 10^{-2}t_o + (-4.44rh^2 + 5.67rh + 1.72)$
$\alpha_{C0,1} (x10^{-1}) = (16.9rh^2 - 16.7rh + 3.96) \times 10^{-3}t_o^2 + (-4.49rh^2 + 4.07rh - 1.0) \times 10^{-1}t_o - 4.68$
$\alpha_{CT,1} = 1.07 \times 10^{-1}$
$A_2 (x10^4s^{-1}) = (12.5rh^2 - 14.8rh + 3.14) \times 10^{-2}t_o^2 + (-4.26rh^2 + 5.11rh - 1.17)t_o + (5.56rh^2 - 7.0rh + 13.7)$
$E_{A2}/R (x10^2K) = (4.80rh^2 - 5.51rh + 1.58) \times 10^{-2}t_o^2 + (-9.24rh^2 + 10.3rh - 3.76) \times 10^{-1}t_o + (2.39rh^2 - 2.85rh - 8.8)$
$m_2 (x10^1) = (4.61rh^2 - 5.37rh + 1.10) \times 10^{-2}t_o^2 + (-15.3rh^2 + 17.6rh - 3.96) \times 10^{-1}t_o + 7.38$



$n_2 = (11.7rh^2 - 14.0rh + 3.10) \times 10^{-3}t_o^2 + (-28.1rh^2 + 38.2rh - 8.63) \times 10^{-2}t_o + 1.94$
$D_2 = (16.3rh^2 - 18.3rh + 5.23) \times 10^{-2}t_o^2 + (7.82rh - 9.94) \times 10^{-1}t_o + (-47.8rh^2 + 56.0rh + 43.7)$
$\alpha_{C0,2} (x10^5) = (-9.06rh^2 - 10.3rh + 1.03) \times 10^{-2}t_o^2 + (1.17rh^2 - 1.12rh - 1.16) \times 10^{-1}t_o + (-2.61rh^2 + 3.28rh - 9.13)$
$\alpha_{CT,2} (x10^3) = (-4.97rh - 4.17) \times 10^{-3}t_o + 1.77$

TABLE S3. Parameters for cure kinetics model for 44DDS (a/e = 0.8)

$A_1 (x10^3s^{-1}) = (-3.25rh + 1.13) \times 10^{-2}t_o^2 + (9.60rh^2 - 9.30rh + 2.16)t_o + (4.0rh + 15.3)$
$E_{A1}/R (x10^{-2}K) = (-28.8rh + 8.20) \times 10^{-2}t_o + (-5.0rh^2 + 5.17rh - 14.4)$
$m_1 (x10^1) = (8.66rh^2 - 11.9rh + 3.71) \times 10^{-2}t_o^2 + (5.55rh - 3.35) \times 10^{-1}t_o + (-3.22rh^2 + 3.53rh - 8.12)$
$n_1 (x10^2) = (3.85rh^2 - 4.86rh + 1.34) \times 10^{-1}t_o^2 + (-8.72rh^2 + 10.4rh - 2.64)t_o + (7.78rh^2 - 8.33rh + 47.5)$
$D_1 (x10^2) = (13.5rh - 3.43) \times 10^{-2}t_o^2 + (5.64rh - 2.18)t_o + (-8.33rh + 136)$
$\alpha_{C0,1} (x10^{-1}) = (1.85rh^2 - 2.45rh + 1.30) \times 10^{-3}t_o^2 + (8.07rh^2 - 9.47rh + 1.88) \times 10^{-1}t_o - 4.85$
$\alpha_{CT,1} = 1.04 \times 10^{-1}$
$A_2 (x10^4s^{-1}) = (10.5rh^2 - 10.4rh + 1.31) \times 10^{-3}t_o^3 + (-45.8rh^2 + 43.0rh - 4.03) \times 10^{-2}t_o^2 + (402rh^2 - 334rh - 2.60) \times 10^{-2}t_o + 6.81$
$E_{A2}/R (x10^2K) = (-42.6rh^2 + 37.9rh - 7.56) \times 10^{-2}t_o^2 + (-19.0rh^2 + 17.2rh - 3.44)t_o + (-3.89rh^2 + 3.43rh - 10.0)$



$m_2 (x10^1) = (-11.5rh+9.58)x10^{-3}t_o^2+(27.7rh^2-31.7rh+5.16)x10^{-1}t_o+(3.44rh^2-3.30rh+7.82)$
$n_2 (x10^1) = (-3.09rh+2.23)x10^{-2}t_o^2+(8.6rh-5.25)x10^{-1}t_o+(6.11rh^2-6.17rh+17.7)$
$D_2 = (8.89rh^2-11.5rh+3.48)x10^{-1}t_o^2+(-3.24rh^2+4.19rh-1.27)x10^1t_o+(4.33rh+52.7)$
$\alpha_{C0,2} (x10^5) = (-17.5rh+7.03)x10^{-2}t_o^2+(7.34rh-2.94)t_o+(3.53rh-9.14)$
$\alpha_{CT,2} (x10^3) = (-4.60rh-4.19)x10^{-3}t_o+1.77$

TABLE S4. Parameters for initial degree of cure ( $\alpha_0$ ) input to cure kinetics model and viscosity model (where  $\alpha_{0,a}$  = actual initial degree of cure (used as an input to viscosity model) and  $\alpha_{0,f}$  = fixed initial degree of cure (= 0.0015, used as an input to cure kinetics model))

$\alpha_{0,a} (33DDS (a/e = 0.6)) = \alpha_{0,f}+(-75.4rh^2+3.24rh+52.0)x10^{-6}t_o^2+(41.3rh^2+13.8rh-1.78)x10^{-4}t_o$
$\alpha_{0,a} (33DDS (a/e = 0.8)) = \alpha_{0,f}+(1.12rh^2-2.39r+1.11)x10^{-4}t_o^2+(-1.74rh^2+9.37rh-1.67)x10^{-3}t_o$
$\alpha_{0,a} (44DDS (a/e = 0.8)) = \alpha_{0,f}+(-31.4rh^2+30.0rh-3.68)x10^{-5}t_o^2+(15.4rh^2+15.0rh+2.61)x10^{-4}t_o$

#### *Viscosity model*

The viscosity ( $\eta$ ) evolution of epoxy resin during processing is affected by two competing effects: temperature and cure. Heating the resin decreases viscosity due to increased molecular mobility, but it also induces cure which increases viscosity due to increase molecular size. To capture these phenomena, along with out-time and moisture absorption effects on  $\eta$  evolution



during cure, a phenomenological model developed by Khoun et al. [20] was adapted and modified to yield the following expression:

$$\eta = \eta_1 + \eta_2 \left( \frac{\alpha_1}{\alpha_1 - \alpha} \right)^{A+B\alpha^d+C\alpha^e} \quad (4)$$

$$\eta_i = A_{\eta_i} \exp \left( \frac{E_{\eta_i}}{RT} \right)_{i=1,2} \quad (5)$$

where  $\eta_i$  is the Arrhenius dependent viscosity component,  $A_{\eta_i}$  is the Arrhenius constant,  $E_{\eta_i}$  is the viscosity activation energy,  $\alpha_1$  is the degree of cure at gelation, and  $A, B, C, d$  and  $e$  are fitting constants. The first term in equation (4) takes an Arrhenius-type form, and the second term is added to account for the rapid viscosity increase near the gelation point. Here, the variables  $A_{\eta_i}, E_{\eta_i}, \alpha_1, A, B, C, d$  and  $e$  were defined as  $f(r, t_o) = g(r)t_o^2 + h(r)t_o + i(r)$  to account for changes associated with ambient temperature cure as well as moisture absorption. The model parameters are provided in Tables S5-S7.

TABLE S5. Parameters for viscosity model for 33DDS ( $a/e = 0.6$ ) (where rh = rh in fraction and  $t_o$  = out-time in days)

$A_{\eta 1} \text{ (x10}^2\text{Pa}\cdot\text{s)} = (-2.07\text{rh}-4.28)\text{x10}^{-1}\text{t}_o+(-8.67\text{rh}+25.1)$
$E_{\eta 1}/R \text{ (x10}^2\text{K)} = (48.3\text{rh}+60.0)\text{x10}^{-2}\text{t}_o+(3.83\text{rh}^2-4.08\text{rh}+122)$
$A_{\eta 2} \text{ (Pa}\cdot\text{s)} = (10.1\text{rh}-2.48)\text{x10}^{-1}\text{t}_o^3+(-43.7\text{rh}+8.05)\text{t}_o^2+(400\text{rh}+13.1)\text{t}_o+326$
$E_{\eta 2}/R \text{ (x10}^1\text{K)} = (-22.8\text{rh}^2+28.8\text{rh}-7.81)\text{x10}^{-3}\text{t}_o^2+(5.83\text{rh}^2-7.14\text{rh}+1.68)\text{x10}^{-1}\text{t}_o+8.47$



$\alpha_1 (x10^1) = (-24.2rh^2+25.4rh-5.01)x10^{-3}t_o^2+(7.17rh^2-7.04rh+1.39)x10^{-1}t_o+4.53$
$A = (22.7rh-9.07)x10^{-3}t_o^2+(-9.55rh+3.82)x10^{-1}t_o+14.2$
$B = (14.7rh^2-17.1rh+3.80)x10^{-1}t_o^2+(-30.0rh^2+33.9rh-7.63)t_o+(20.0rh^2-23.7rh+60.7)$
$C = (-16.2rh^2+19.1rh-4.44)x10^{-1}t_o^2+(34.6rh^2-39.6rh+9.49)t_o+(-25.6rh^2+31.7rh-63.8)$
$d (x10^2) = (2.10rh-3.30)x10^{-2}t_o^2+(-2.73rh+8.10)x10^{-1}t_o+(1.72rh-7.51)$
$e (x10^5) = (12.0rh-3.43)x10^{-2}t_o^2+(-5.11rh+1.48)t_o+(-1.67rh+137)$

TABLE S6. Parameters for viscosity model for 33DDS (a/e = 0.8) (where rh = rh in fraction and t<sub>o</sub> = out-time in days)

$A_{\eta 1} (x10^2Pa \cdot s) = (-14.3rh+5.26)x10^{-2}t_o^2+(4.29rh-1.15)t_o+(-11.8rh^2+15.1rh-4.10)$
$E_{\eta 1}/R (K) = (-7.10rh^2+8.62rh-1.95)x10^{-2}t_o^2+(21.3rh^2-25.8rh+5.77)x10^{-1}t_o+1.41$
$A_{\eta 2} (x10^{-1}Pa \cdot s) = (-1.78rh^2+1.97rh+4.63)t_o^2+(4.44rh^2-5.0rh-20.1)x10^1t_o+1.93x10^3$
$E_{\eta 2}/R (x10^1K) = (15.0rh^2-18.0rh+3.96)x10^{-2}t_o^2+(-4.19rh^2+5.06rh-1.07)t_o+(-1.78rh^2+2.53rh+6.52)$
$\alpha_1 (x10^2) = (-12.2rh+6.98)x10^{-2}t_o^2+(4.14rh-2.16)t_o+(-2.50rh+60.3)$
$A = (-9.94rh+2.16)x10^{-3}t_o^2+(29.3rh-5.17)x10^{-2}t_o+14.1$
$B = (3.14rh-2.62)x10^{-1}t_o^2+(-11.4rh-10.0)t_o+(-1250rh^2+1700rh-1.0)x10^{-1}$



$C = (-3.59rh+2.84) \times 10^{-1}t_o^2 + (12.6rh-10.6)t_o + (124rh^2-171rh+4.0)$
$d (x10^4) = (-4.50rh^2+5.58rh-2.46)t_o + (-6.83rh+18.1)$
$e (x10^2) = (5.09rh-1.87) \times 10^{-3}t_o^2 + (-15.1rh+2.76) \times 10^{-2}t_o + (1.67rh^2-2.17rh+1.71)$

TABLE S7. Parameters for viscosity model for 44DDS (a/e = 0.8) (where rh = rh in fraction and t<sub>o</sub> = out-time in days)

$A_{\eta 1} (x10^3 Pa \cdot s) = (2.80rh+6.12) \times 10^{-1}t_o^2 + (-5.67rh-28.5)t_o + (6.67rh+286)$
$E_{\eta 1}/R (x10^2 K) = (-69.7rh+3.60) \times 10^{-3}t_o^2 + (16.0rh+6.07) \times 10^{-1}t_o + (-3.33rh+125)$
$A_{\eta 2} (x10^{-2} Pa \cdot s) = (-7.22rh^2+9.50rh+3.84)t_o^2 + (2.06rh^2-2.75rh-2.0) \times 10^2t_o + (5.0rh+262) \times 10^1$
$E_{\eta 2}/R (x10^2 K) = (5.38rh^2-6.45rh+1.45) \times 10^{-1}t_o^2 + (-12.3rh^2+16.2rh-3.26)t_o + (-3.89rh^2+5.17rh+64.0)$
$\alpha_1 (x10^2) = (1.91rh-1.03)t_o + (-6.83rh+66.7)$
$A = (-7.29rh+1.84) \times 10^{-3}t_o^2 + (16.4rh+1.87) \times 10^{-2}t_o + 13.0$
$B = (-14.4rh^2+19.8rh-6.59) \times 10^{-1}t_o^2 + (45.3rh^2-60.0rh+19.3)t_o + (7.33rh+59.3)$
$C = (13.6rh^2-18.8rh+6.27) \times 10^{-1}t_o^2 + (-42.1rh^2+56.0rh-18.3)t_o + (-8.0rh-54.3)$
$d (x10^3) = (-2.17rh^2+3.08rh-5.13) \times 10^{-3}t_o^2 + (7.22rh^2-9.83rh+20.3) \times 10^{-2}t_o - 1.61$
$e (x10^3) = (16.4rh^2-22.0rh+2.05) \times 10^{-1}t_o^2 + (-511rh^2+657rh+8.0) \times 10^{-1}t_o + (-5.0rh-159)$



## RESULTS AND DISCUSSION

### *Out-time characterization*

Previous studies have shown that out-time or aging-induced cross-linking of the epoxy resin causes  $\alpha_0$  to increase, and the moisture absorbed during out-time can affect the reaction by acting as both catalyst and solvent [10-15]. To verify this, TGA was used to monitor mass stability during heating and results were measured. Fig. 2(a) compares the weight percent of absorbed water change with out-time for resin systems with the same cure agent (33DDS) but different a/e stoichiometric ratio. The data show that the water uptake increases with rh and with higher a/e stoichiometric ratio.

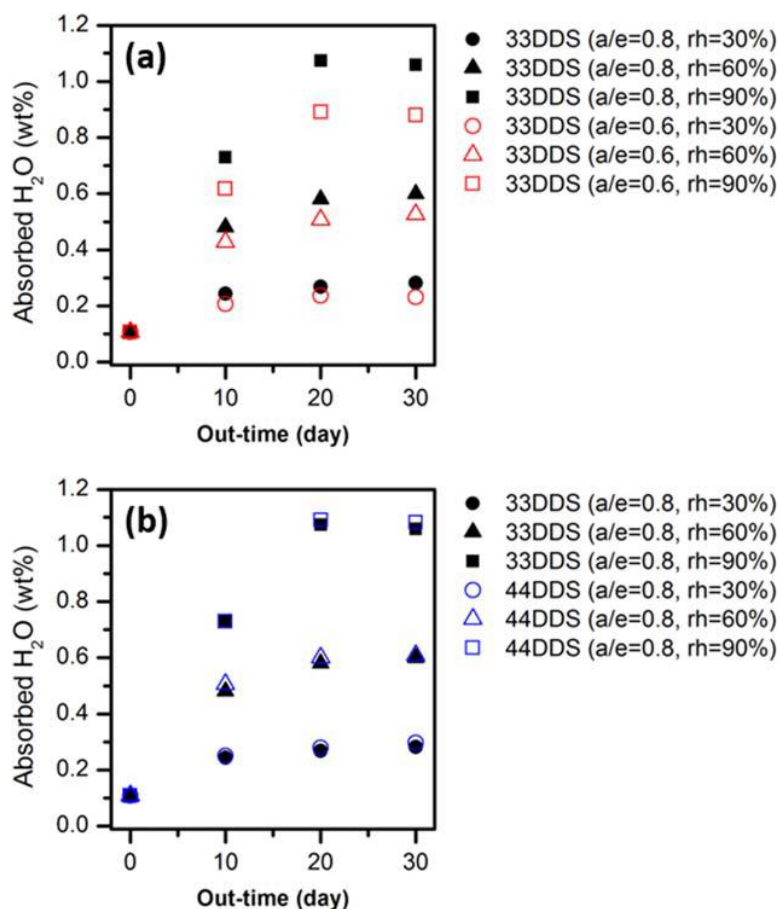






FIG. 2. Weight percent of absorbed water ( $H_2O$ ) change on out-time and rh for: (a) 33DDS ( $a/e = 0.8$ ) and 33DDS ( $a/e = 0.6$ ); and (b) 33DDS ( $a/e = 0.8$ ) and 44DDS ( $a/e = 0.8$ ).

Fig. 2(b) shows the water uptake as a function of out-time for formulations with different isomeric cure agents but identical  $a/e$  stoichiometric ratios. The data show that water absorption is a strong function of rh and of the amount of available amine groups in the resin. Both 33DDS and 44DDS based resins exhibit nearly the same water absorption level across all out-time values at each different rh conditioning. Thus, combined, the results in Fig. 2 indicate that amine has greater affinity towards the hydroxyl group in water than to the epoxy group. Furthermore, water absorption is a weak function of the ‘ambient temperature-induced’ primary degree ( $1^\circ$ ) amine-epoxy reaction (or  $\alpha_0$ ), which is expected to progress until the resin  $T_g$  approaches the ambient temperature, where it vitrifies. At equilibrium, for resins with  $a/e = 0.8$ , roughly 1.1 wt% water was absorbed for a rh of 90%, while only 0.2 wt% was absorbed for the resin with  $a/e = 0.6$ . Thus, at a molecular level, we expect that samples conditioned at higher humidity levels will exhibit greater changes in  $\alpha_0$  associated with the catalytic and solvent effect.

$\Delta H_T$  of the resin was determined by integrating the exothermic heat flow evolution from DSC heating measurements where the resin was fully cured. The  $\alpha_0$  was calculated using the equation:

$$\alpha_0 = \frac{\Delta H_T(day0) - \Delta H_T(out-time)}{\Delta H_T(day0)} \quad (6)$$



where  $\Delta H_T$  is expected to decrease with out-time due to the decrease in the number of reactants. Values of  $\alpha_0$  are plotted in Fig. 3. For the convenience of modelling cure kinetics and viscosity evolution during cure, the  $\alpha_0$  change on out-time can be fitted as:

$$\alpha_{0,a} = \alpha_{0,f} + \alpha_{0,v}(t_o, rh) \quad (7)$$

where  $\alpha_{0,a}$  is actual initial degree of cure (used as an input to the  $\eta$  model),  $\alpha_{0,f}$  is the fixed initial degree of cure (= 0.0015, a fixed fitting parameter used as an input to the cure kinetics model), and  $\alpha_{0,v}$  is variable degree of cure. The model parameters determined are provided in Table S4. The results show that for all resin types,  $\alpha_0$  increases with out-time in a predictable manner. Resin conditioned at higher rh levels exhibited a sharper increase in  $\alpha_0$ , as absorbed water facilitated cross-linking at the ambient temperature.

Fig. 3(a) shows that 33DDS with higher a/e stoichiometric ratio ages more rapidly, presumably due to higher collision numbers between available amine and epoxy group. Resins with the same a/e stoichiometric ratio but with different isomeric cure agents are compared in Fig. 3(b), and the data show that 33DDS (with meta substitution)-based resins age substantially more rapidly than the 44DDS (with para substitution)-based resins. The accelerated aging occurs because the reactivity of the amine depends upon the nucleophilicity of the amino group [7]. Both 33DDS and 44DDS isomers have the same electron withdrawing sulphonyl group, where the only difference comes from the orientation of the  $\text{NH}_2$  groups. Due to para-substitution, 44DDS has delocalization of the lone pairs of electrons on nitrogen but such resonance is not possible in meta-substitution, 33DDS. Consequently, 33DDS is more reactive with epoxide groups than 44DDS.

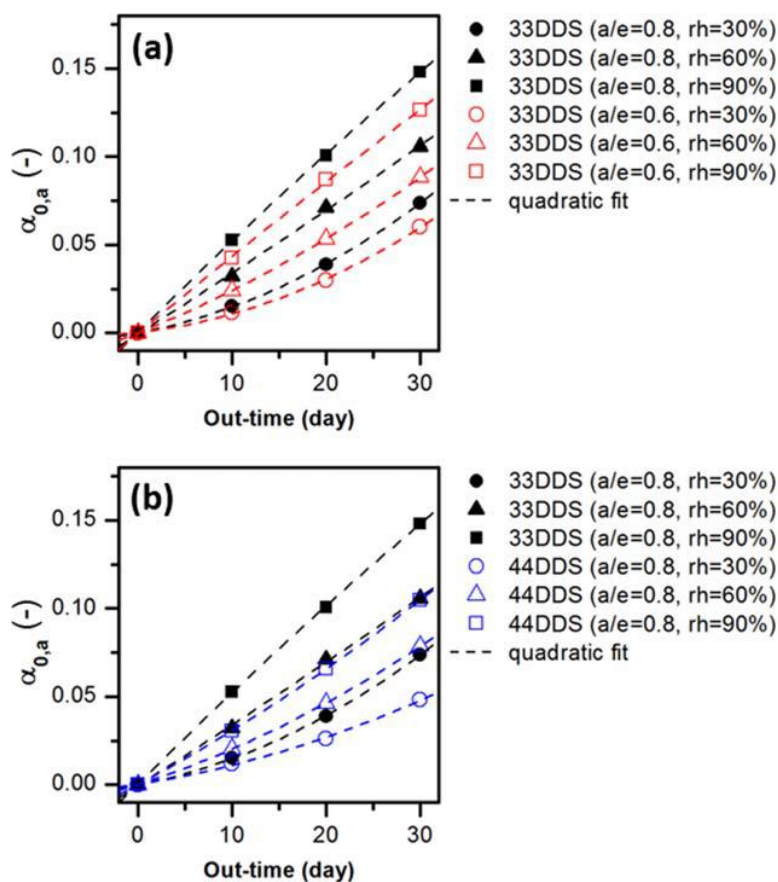


FIG. 3. Dependence of initial degree of cure ( $\alpha_{0,a}$ ) on out-time and rh for: (a) 33DDS ( $a/e = 0.8$ ) and 33DDS ( $a/e = 0.6$ ); and (b) 33DDS ( $a/e = 0.8$ ) and 44DDS ( $a/e = 0.8$ ).

The effects of absorbed moisture on the B-stage or initial glass transition temperature ( $T_{g,0}$ ) during out-time were determined from MDSC data and are displayed in Fig. 4. Measurement of  $T_{g,0}$  requires moderate heating of the sample, usually to slightly above ambient temperature, making it useful for tracking out-time. Fig. 4(a) shows that nearly the same  $T_{g,0}$  values are obtained for 33DDS-based resins conditioned at the same rh but with different  $a/e$  stoichiometric ratios, except at day 30. The resin with higher  $\alpha_0$  is expected to have higher  $T_{g,0}$ . The results manifest the presence of two competing effects, where the solvent effect of water decreases  $T_{g,0}$ , while the



catalytic effect of water together with the higher a/e stoichiometric ratio provide higher collision numbers, thus increasing  $T_{g,0}$ . These competing effects are also apparent in Fig. 4(b), where the 44DDS based resin aged at 60 & 90% rh exhibits a decrease in  $T_{g,0}$  at day 10, despite progression towards a higher  $\alpha$ .

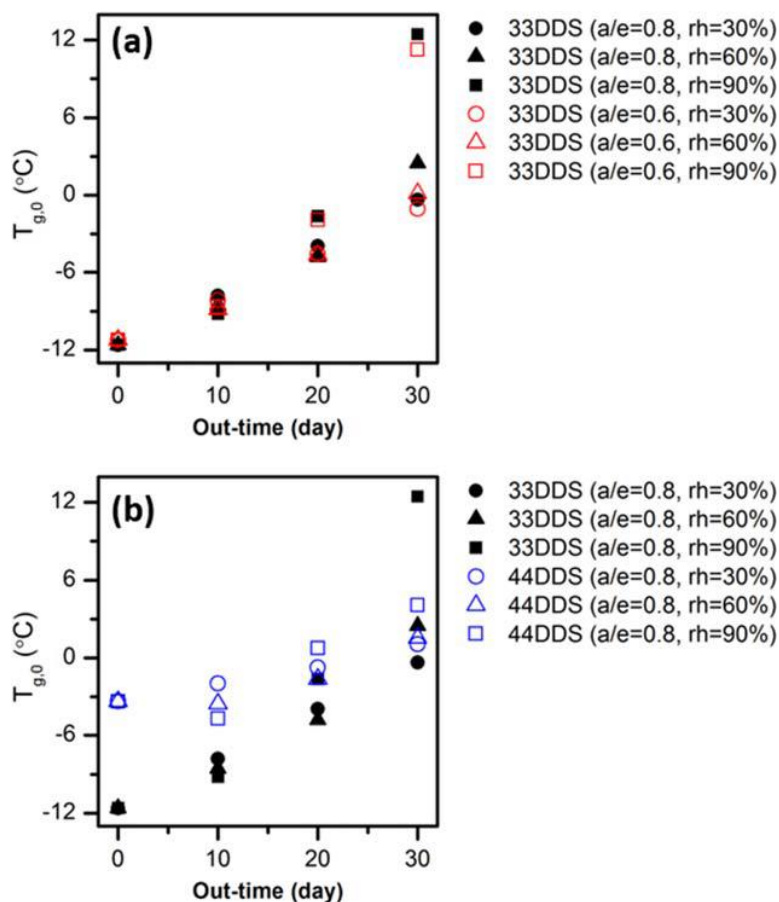


FIG. 4. Initial glass transition temperature ( $T_{g,0}$ ) dependence on out-time and rh for: (a) 33DDS (a/e = 0.8) and 33DDS (a/e = 0.6); and (b) 33DDS (a/e = 0.8) and 44DDS (a/e = 0.8).

When the 33DDS-based resin is fully cured, it will have greater configurational entropy than the 44DDS-based resins, making the resin more flexible and resulting in lower  $T_g$ . Out-time and rh conditioning effects here show that 44DDS-based resins exhibit higher  $T_{g,0}$  than the



33DDS-based resins until day 20, despite 44DDS based resin having lower  $\alpha_0$  (see Fig. 3(b)). With continued aging, the result reverses for day 30 samples conditioned at  $rh = 60$  &  $90\%$ , where  $\alpha_0$  further increases quadratically and more rapidly against out-time for the 33DDS-based resin relative to the 44DDS-based resin. Thus, tracking evolution of  $T_{g,0}$  may not be a reliable way to track  $\alpha_0$  for a resin exposed to variable environmental conditions. Overall, the combination of out-time and moisture absorption leads to permanent changes in the resin state prior to cure, and this is expected to affect the course of cure kinetics and viscosity evolution during cure.

### *Cure kinetics evolution and modelling*

Fig. 5 shows representative cure kinetics measurements and the corresponding predictive model obtained using equation (2). Note that  $\alpha$  is an integration of cure rate over time, and thus only the cure rate results are presented here. Cure kinetics data and the model results for fresh resin and resin conditioned at  $rh = 90\%$  for 30 days provide two extremities in terms of the cure kinetics change/shift and thus were chosen to demonstrate the model's accuracy. Thus, these quantities have been selected and are plotted in Fig. 5, and the parameters for the cure kinetics models are shown in Table S1-S3. The cure kinetics model for each resin system was first developed using isothermal dwell data at  $121$  and  $150$  °C, and dynamic ramp data with fresh resin samples. Subsequently, isothermal dwells at  $150$  °C and dynamic ramps were conducted on all three resin systems conditioned at  $RH = 30, 60$  and  $90\%$  from  $0$  to  $30$  days. These conditions were selected to take into account the effects of moisture absorption and out-time during cure, and to determine parameters in the cure kinetics equation. Confining the parameters to predictable patterns as



functions of out-time and rh, the present cure kinetics model captured out-time and humidity effects accurately over the entire range of conditions studied.

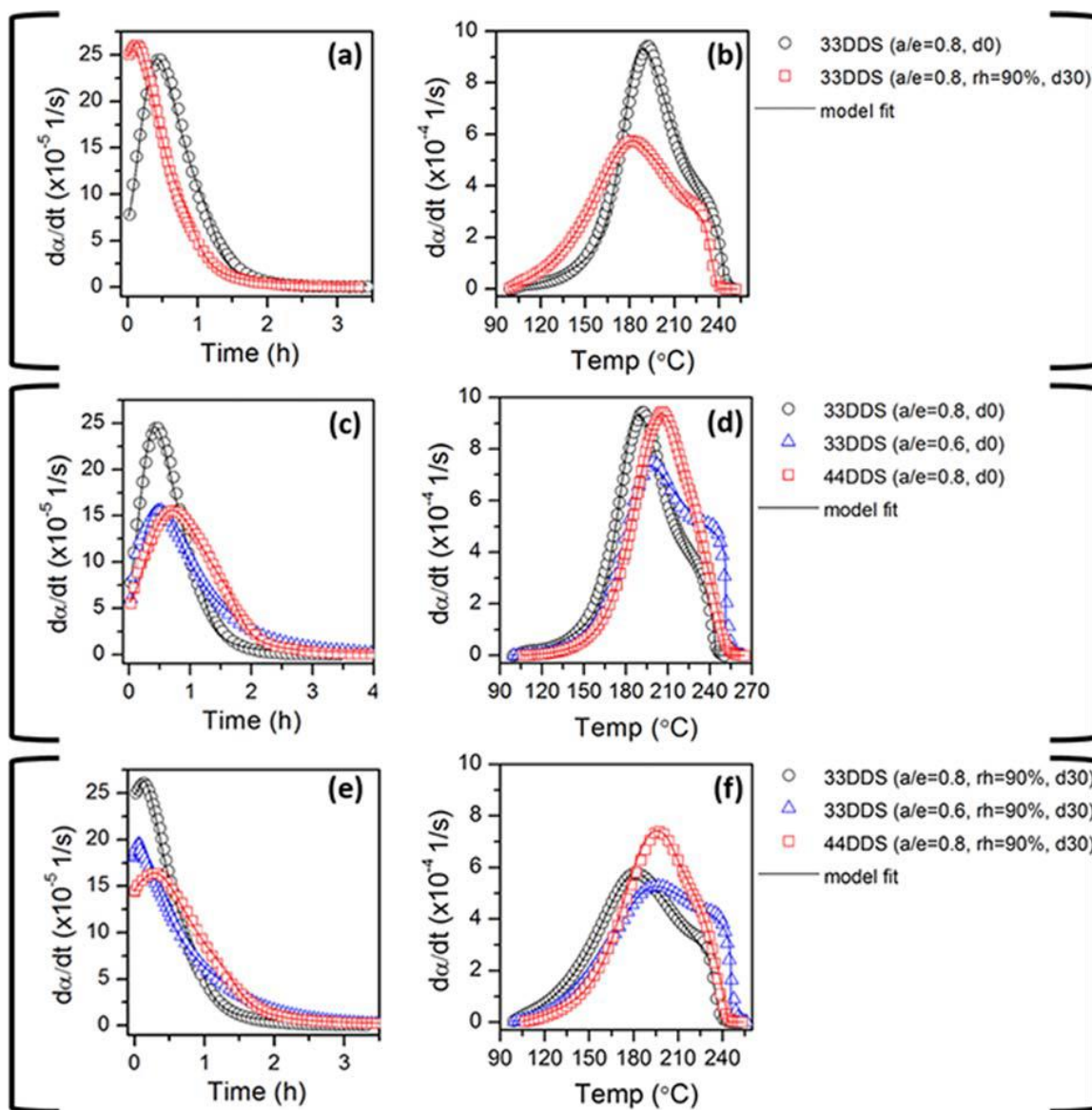


FIG. 5. Representative cure kinetics measurement and model prediction of isothermal dwell and dynamic ramp.



Out-time induced cross-linking causes  $\alpha_0$  to increase, and absorbed moisture can further catalyze this reaction. In general, the thermoset resin cure can be perceived as a blend of fast- and slow-occurring reactions, which are kinetics-driven and diffusion-driven, respectively. Thus, out-time, where the reaction is induced at ambient temperature, is expected to mainly affect kinetically driven reactions. Such reaction will proceed until the resin reaches its  $T_g$ , at which point the resin vitrifies.

Overall, time-based (horizontal axis) cure rate shifts are more apparent during isothermal cure than during dynamic ramp conditions, as the reaction temperature is relatively high. On the other hand, magnitude-based cure rate shifts with out-time and rh conditioning are more apparent under dynamic ramp conditions. Both time- and magnitude-based shifts are greater with higher a/e stoichiometric ratios within the same cure agent, and weaker with para-substituted 44DDS-based resin, as it exhibits slower cure rates than the meta-substituted 33DDS-based resin.

### *Viscosity evolution and modelling*

Fig. 6 shows representative  $\eta$  measurements and the corresponding predictive model obtained using equation (4). As with the development of the cure kinetics model, fresh resin samples were used to generate isothermal dwell data at 121 and 150 °C, and these data were then combined with dynamic ramp data to develop a benchmark viscosity model. Subsequently, resin samples conditioned at rh = 30, 60 and 90% from 0 to 30 days were used to account for the effects of moisture absorption and out-time during cure and to determine parameters in the  $\eta$  equation. Parameters for  $\eta$  models are shown in Tables S5-S7. Fig. 6 shows that the viscosity model captured out-time and humidity effects accurately over the entire range of conditions studied.

Please cite the article as: D. Kim, and S.R. Nutt, “**Processability of DDS Isomers-Cured Epoxy Resin: Effects of Amine/Epoxy Ratio, Humidity, and Out-Time**” Polymer Engineering and Science. 2017. DOI: **10.1002/pen.24738**



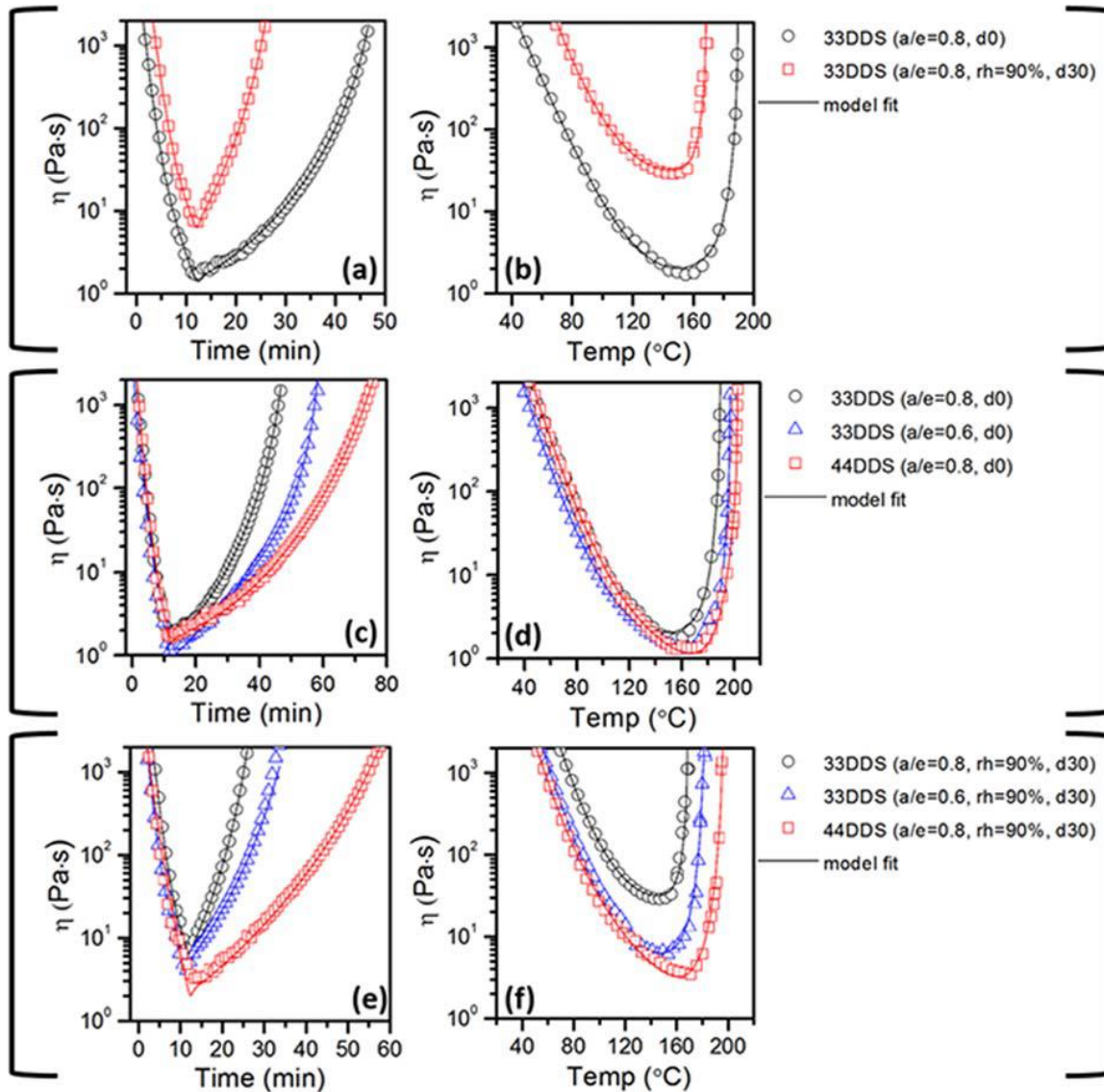


FIG. 6. Representative viscosity ( $\eta$ ) measurements and model prediction of isothermal dwells and dynamic ramps.

Generally,  $\eta$  evolution for a cure cycle is governed by the competing effects of cure (which increases  $\eta$ ) and heating (which decreases  $\eta$ ). Initially, as the temperature increases and the





resin degree of cure is low, the thermal effect is predominant, and the  $\eta$  decreases. As the  $\alpha$  begins to accelerate and the temperature approaches the isothermal dwell, the process becomes cure-driven, and the  $\eta$  increases at an increasing rate until gelation occurs, where the resin flow decreases drastically. Such effects are apparent in Fig. 6. In addition, the  $\eta$  also increases with ambient exposure, moisture absorption, and cure. The phenomena are especially important because viscosity directly affects resin flow, and the deviation from Newtonian behavior is expected near the gel point ( $G' = G''$  [21]), or the flow stop point. In other words, the  $\eta$  levels and resin flow times required to completely wet fiber tows during prepreg processing are progressively limited by ambient temperature, moisture absorption, and cure. Therefore, the increase in  $\eta$  due to ambient exposure and moisture absorption is the primary factor that determines resin out-life, as specified by resin manufacturers.

Comparing the same 33DDS-based resin with different a/e stoichiometric ratios, a lower a/e stoichiometric ratio offers a lower  $\eta$  profile when subjected to the same cure cycle, while the 44DDS-based resin exhibits an even lower  $\eta$  profile. This behavior arises because under the same cure cycle, cure progresses most rapidly in 33DDS with a/e = 0.8, and most slowly in 44DDS with a/e = 0.8. Furthermore, this effect is more pronounced under dynamic ramps. Therefore, in designing epoxy resins for prepreg, consideration must include the effect of reaction speed on flow level and flow duration, as these are critical to full impregnation during processing, as well as the effects of out-time and rh conditioning. As demonstrated in a previous study [10], an accurate model for viscosity allows one to develop a viscosity-controlled (or flow-enhanced) cure cycle that can in principle extend out-life and limit flow-induced defects, while also minimizing cycle time for prepreg.



### *Gelation point*

For epoxies, gelation is often defined as the point where  $G'$  and  $G''$  intersect [18] (Fig. 7(a)). At gelation,  $\eta$  increases quickly, cure effects dominate over thermal effects, and deviation from Newtonian behavior is expected [22]. Thus, gelation is also the flow stop point. In other words, the viscosity levels and resin flow times required to completely wet fiber tows during processing are progressively limited by ambient temperature, moisture absorption, and cure. Therefore, the increase in viscosity due to ambient exposure and moisture absorption is the primary factor that determines the out-time limit or out-life for prepreg.

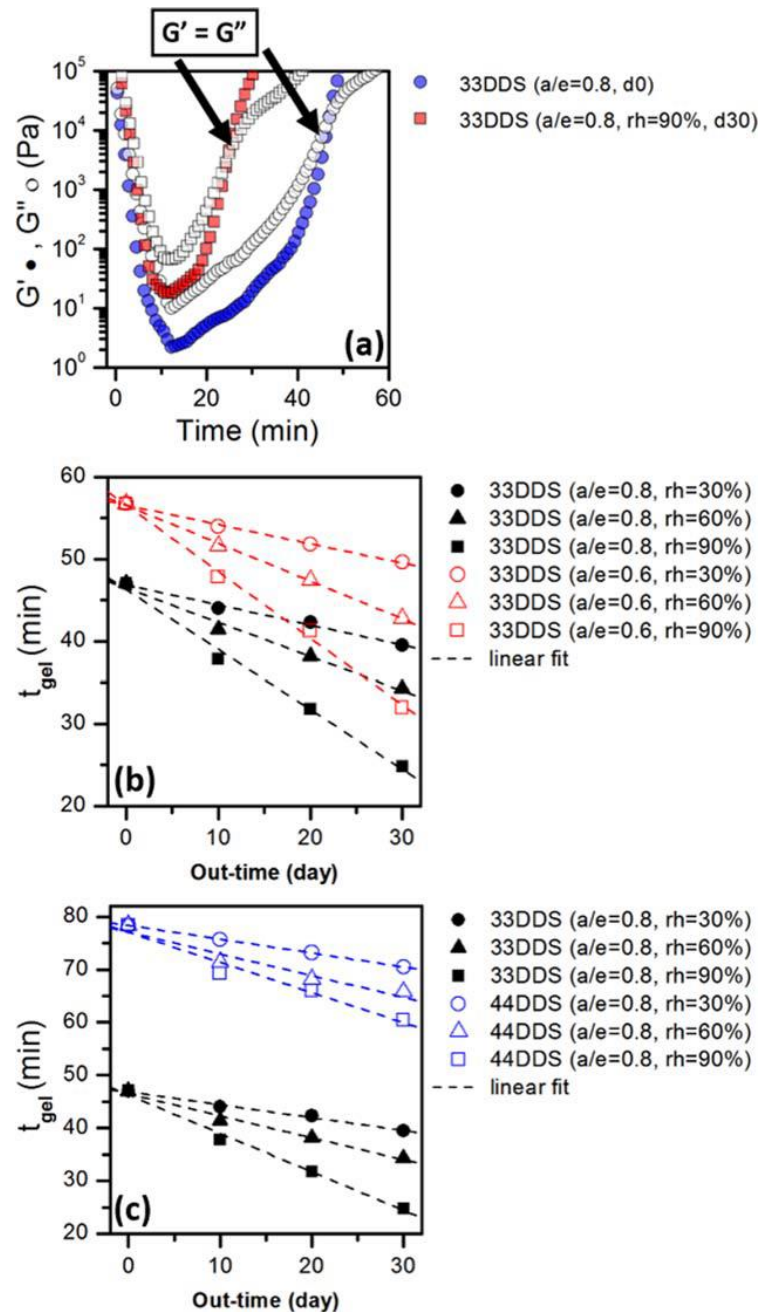


FIG. 7. Gelation time ( $t_{gel}$ ) measurement method and change under isothermal dwell. (a)  $G'$  and  $G''$  versus cure time for 33DDS resin with  $a/e = 0.8$  (b)  $t_{gel}$  versus out-time for 33DDS resin with  $a/e = 0.6$  and  $0.8$  (c)  $t_{gel}$  versus out-time for 33DDS resin and 44DDS resin with  $a/e = 0.8$ .



As expected, Fig. 7(b) & (c) show that for all resin systems,  $t_{gel}$  or ‘resin flow time’ under similar cure conditions decreases with both out-time and higher rh conditioning. The 33DDS resin with  $a/e = 0.6$  exhibits higher  $t_{gel}$  than 33DDS with  $a/e = 0.8$ , as the reaction is slower. Comparing para-substituted 44DDS resin and meta-substituted 33DDS resin, the reaction of the 44DDS resin is substantially slower than the 33DDS resin and attains a lower  $\alpha_0$  during out-time and humidity conditioning. As a result, the 44DDS resin exhibits a  $t_{gel}$  nearly twice that of the 33DDS resin. Thus, from the perspective of a resin formulator, 44DDS and lower  $a/e$  stoichiometric ratios offer longer  $t_{gel}$  and thus longer resin flow time. The epoxy resin flow stops at the gelation point, yet the resin may still continue to react.

#### *Glass transition temperature*

Glass transition or vitrification point is determined using MDSC from the inflection point of the heat capacity ( $C_p$ ) during the isothermal dwell period [22]. The results, tabulated in Table 1, show that for a given resin system, during isothermal dwells, where etherification reaction is unlikely to occur, higher  $a/e$  stoichiometric ratios resulted in higher  $T_g$  values, as these formulations have more amine-epoxy bonds. However, due to etherification at higher temperature, fully cured  $T_g$  (or  $T_{g,\infty}$ ) reached nearly the same level. Comparing para-substituted 44DDS resin and meta-substituted 33DDS resin, the  $T_g$  of 33DDS-based resin was lower, because 33DDS resin has greater configurational entropy, making the resin more flexible and yielding lower  $T_g$ .



TABLE 1. Glass transition temperature ( $T_g$ ) for all resin systems where  $T_{g,121C}$  and  $T_{g,150C}$  are  $T_g$  for resins cured at isothermal dwell of 121 °C and 150 °C respectively and  $T_{g,\infty}$  is  $T_g$  for fully cured resin.

	33DDS (a/e = 0.8)	33DDS (a/e = 0.6)	44DDS (a/e = 0.8)
$T_{g,121C}$ (°C)	145.9	139.9	148.3
$T_{g,150C}$ (°C)	182.7	175.5	191.6
$T_{g,\infty}$ (°C)	216.4	215.8	236.8

### *Resin flow control*

The cure kinetics measurements,  $\eta$  measurements, and predictive models developed in this study show that the influence of out-time and absorbed moisture on the resin viscosity can be substantial. This, in turn, can cause incomplete impregnation of resin on fiber beds during prepreg processing. However, with the predictive  $\eta$  model developed here, the temperature cycle can be tuned to potentially develop a flow-enhanced or viscosity-controlled cure cycle that can limit flow induced defects.

A squeezing flow geometry have been widely investigated for characterizing resin flow during lamination [1, 23-24]. Here, the prepreg layup is sandwiched between stainless steel plates into the Instron test frame, where a linear variable differential transformer is used to measure the movement of the cross heads. While the plates are heated, a constant force is applied and measured

Please cite the article as: D. Kim, and S.R. Nutt, “**Processability of DDS Isomers-Cured Epoxy Resin: Effects of Amine/Epoxy Ratio, Humidity, and Out-Time**” Polymer Engineering and Science. 2017. DOI: **10.1002/pen.24738**



by the load cell. Assuming that the resin flow can be approximated as Newtonian before it gels, a characteristic flow quantity called flow number ( $N_{FL}$ ) has been defined as follows:

$$N_{Fl} = \left( \frac{\rho_p}{\rho_o} \right) \left[ 1 - \left( \left[ \frac{16Fh_o^2}{3\pi R^4} \int_0^{t_{gel}} \eta(t)^{-1} dt \right] + 1 \right)^{-0.5} \right] \cdot 100 \quad (7)$$

where  $\rho_p$  is the resin density,  $\rho_o$  is the prepreg density,  $F$  is the lamination press force,  $h_o$  is the initial stack thickness,  $R$  is the effective radius of the resin. The main variable controlling the flow quantity is:

$$N_{Fl,eff} = \int_0^{t_{gel}} \eta(t)^{-1} dt \quad (8)$$

where  $N_{FL,eff}$  is the effective flow number, and higher  $N_{FL,eff}$  means more resin flow. With the predictive  $\eta$  model developed in this study, there are two controlling variables that affect  $\eta$  evolution: heating rate and dwell temperature. Fig. 8 compares  $\eta$  evolution at various dwell temperatures and heating rates. The  $\eta$  evolution during cure is primarily affected by cure temperature and  $\alpha$ , where an increase in temperature leads to decrease in  $\eta$ , yet it also accelerates cure, which increases  $\eta$ . Additionally, higher heating rate leads to a more rapid decrease in  $\eta$ , allowing the resin to achieve lower  $\eta$  before the substantial effect of cure kicks in. However, once the resin reaches cure temperature, the rapid cure effect is expected, thus leading to reduction in resin flow time.

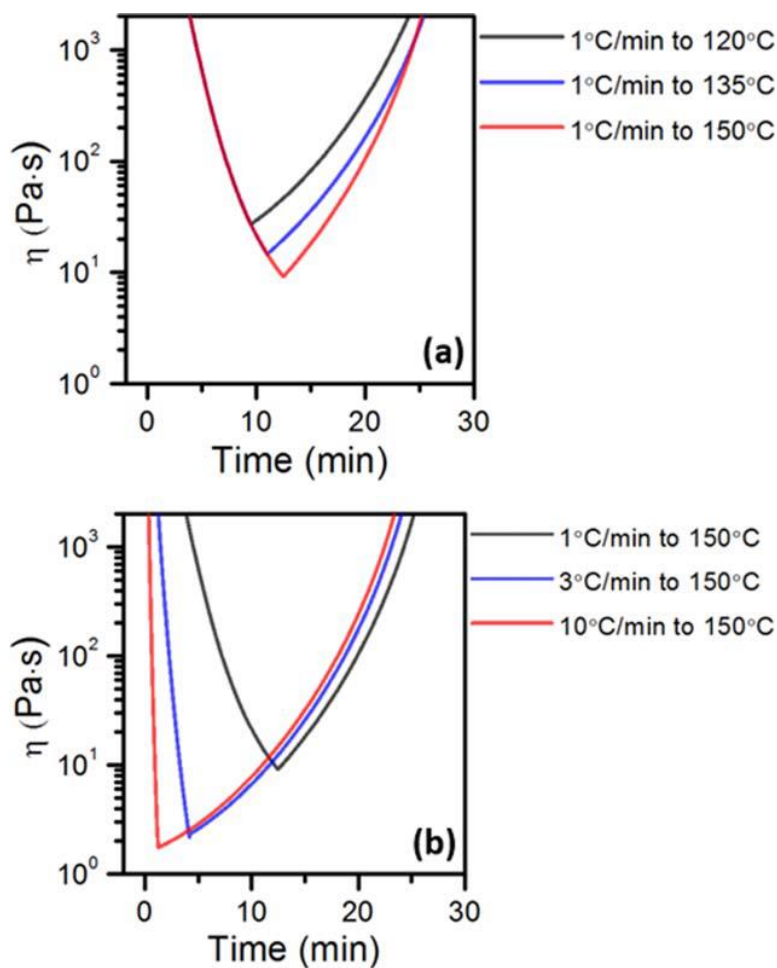


FIG. 8.  $\eta$  model prediction for 33DDS ( $a/e = 0.8$ , rh 90%) at day 30: (a) fixed ramp rate to incremental dwell temperatures and (b) incremental ramp rate to the same dwell temperature.

These competing effects are evident in Fig. 8, where  $\eta$  model prediction for 33DDS ( $a/e = 0.8$ , rh 90%) at day 30 were subjected to various heating rates and dwell temperatures. The results show that a higher dwell temperature leads to lower  $\eta$ , yet the faster cure effect leads to a more rapid  $\eta$  increase (Fig. 8(a)). Also, a more rapid heating rate is shown to lead to lower  $\eta$ , although once the temperature reaches the dwell temperature, which occurs at around the  $\eta_{min}$ ,  $\eta$  is shown to increase at the same rate regardless of thermal history. Fig. 9 depicts  $N_{FL,eff}$  calculated using



equation (8) at various cure conditions. The purpose of this analysis was not to find a maximum  $N_{FL,eff}$ , although it is apparent that the predictive  $\eta$  model allows design of a ‘flow-enhanced’ cure cycle that is specific to the particular resin system, aging, and thermal history.

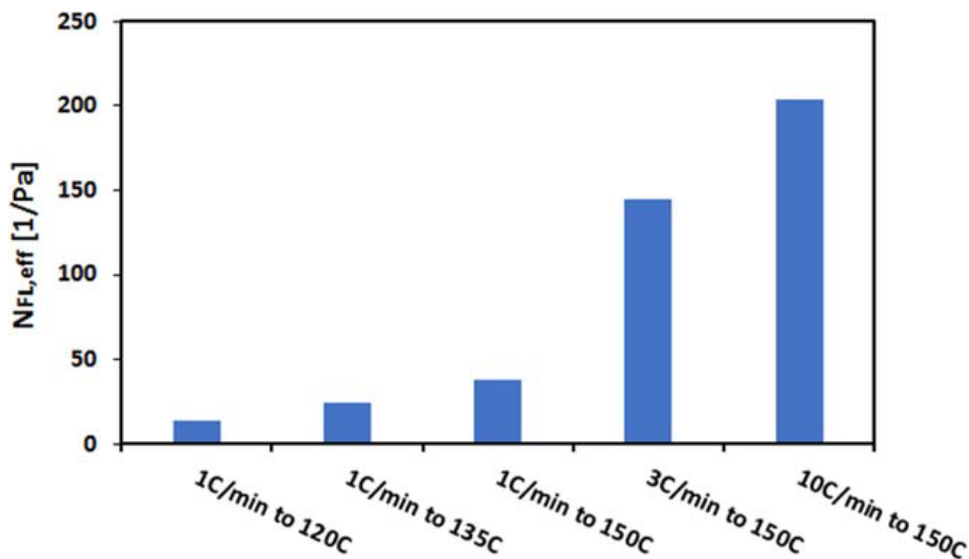


FIG. 9. Effective flow number ( $N_{FL,eff}$ ) at various cure conditions for 33DDS ( $a/e = 0.8$ ,  $rh = 90\%$ ) at day 30.

## CONCLUSIONS

Three aerospace grade resins were formulated to investigate the effects of variation in DDS isomers,  $a/e$  stoichiometric ratio, out-time, and moisture absorption on processing characteristics and cured resin properties. First, conventional thermochemical and thermomechanical methods (MDSC and rheometry) were used to collect benchmark data. Regardless of the resin system, the results show that out-time increases initial degree of cure and more so with moisture absorption which influence the cure kinetics and viscosity evolution during cure. These effects, in turn, will





shorten flow level and time which could potentially lead to insufficient resin flow during composite manufacturing. Therefore, limiting out-time and including humidity and thermal controls are generally required to ensure sufficient resin flow.

Then, accurate process models were developed that comprehensively capture out-time and humidity effects on cure kinetics and viscosity for each resin systems. Among the three resin systems investigated in this study, meta- substituted 33DDS with  $a/e = 0.8$  exhibited the highest cure rate and the lowest flow time. This behavior was attributed to the increase in collision number between amine and epoxy compared to  $a/e = 0.6$  and the lack of delocalization of the lone pair of electrons on nitrogen compared to para- substituted 44DDS. Conversely, 44DDS with  $a/e = 0.8$  exhibited the slowest cure rate with the highest flow time. In addition, 44DDS based resin exhibited the highest glass transition temperature due to having lower configurational entropy than 33DDS based resin. The results offer practical insights regarding resin formulation and prepreg processing, particularly that: (1) 33DDS-based resin is more susceptible to aging and flow time reduction, albeit with faster processing time; (2) lower  $a/e$  will require longer dwell at higher temperature to complete the etherification reaction, albeit with more flow time; and (3) 44DDS resin offers longer flow time with higher glass transition temperature, yet with substantially longer processing time. Finally, the predictive viscosity model demonstrates a method to enhance resin flow during prepreg processing which can potentially limit flow-induced defects.

Overall, this study provides foundational knowledge for aerospace grade DDS isomer cured resins subjected to pre-cure conditions that are largely unavoidable in practice with prepreg processing. The predictive models developed here can be used to enhance resin flow. The models combined with the experimental results, they potentially allow adaptive manufacturing of quality parts with non-ideal material and process conditions.

Please cite the article as: D. Kim, and S.R. Nutt, **“Processability of DDS Isomers-Cured Epoxy Resin: Effects of Amine/Epoxy Ratio, Humidity, and Out-Time”** Polymer Engineering and Science. 2017. DOI: **10.1002/pen.24738**



## ACKNOWLEDGEMENTS

The authors acknowledge financial support from the M.C. Gill Composites Center and the Airbus Institute for Engineering Research at USC. The resins used in this study were generously donated by Huntsman Co., and Sumitomo Chemical Co.; and consumables were donated by Airtech International Inc. The authors acknowledge Dr. Jack Boyd for helpful discussions.

## REFERENCES

1. A V. Tungare , G.C. Martin, and J.T. Gotro, *Polym. Eng. Sci.*, **28**, 1071 (1988).
2. F.G. Garcia, B.G. Soares, V.J. Pita, R. Sanchez, and J.J. Rieumont, *Appl. Polym. Sci.*, **106**, 1457 (2007).
3. S. Swier, and S.S. Mele, *J. Polym. Sci. Pol. Phys.*, **41**, 594 (2003).
4. M.S. Vratsanos, and R.J. Farris, *Polym. Eng. Sci.*, **29**, 806 (1989).
5. M.R. Vanlandingham, R.F. Eduljee, and J.W. Gillespie, *J. Appl. Polym. Sci.*, **71**, 699 (1999).
6. T.D. Chang, S.H. Carr, and J.O. Brittain, *J. Polym. Eng. Sci.*, **22**, 1213 (1989).
7. I.K. Varma, and P.V. Satya Bhamu, *J. Compos.Mater.*, **20**, 410 (1986).
8. B.G. Min, Z.H. Stachurski, and J.H. Hodgkin, *Polymer.*, **34**, 4488 (1993).
9. C.L. Bongiovanni, and J.D. Boyd, U.S. Patent, 2010/0222461, (2010).

Please cite the article as: D. Kim, and S.R. Nutt, “**Processability of DDS Isomers-Cured Epoxy Resin: Effects of Amine/Epoxy Ratio, Humidity, and Out-Time**” *Polymer Engineering and Science*. 2017. DOI: **10.1002/pen.24738**



10. D. Kim, T. Centea, and S.R. Nutt, *Compos. Sci. Technol.*, **138**, 201 (2017).
11. M. Jackson, M. Kaushik, S. Nazarenko, S. Ward, R. Maskell, and J. Wiggins, *Polymer.*, **52**, 4528 (2011).
12. S. Alessi, E. Caponetti, O. Güven, M. Akbulut, G. Spadaro, and A. Spinella, *Macromol. Chem. Phys.*, **216**, 538 (2015).
13. G. Pitarresi, M. Scafidi, S. Alessi, M. Di Filippo, C. Billaud, and G. Spadaro, *Polym. Degrad. Stabil.*, **111**, 55 (2015).
14. R.W. Jones, Y. Ng, and J.F. McClelland, *Compos. Part A Appl. Sci. Manuf.*, **39**, 965 (2008).
15. L.K. Grunenfelder, T. Centea, P. Hubert, and S.R. Nutt, *Compos. Part A Appl. Sci. Manuf.*, **45**, 119 (2013).
16. M.C. Kazilas, and I.K. Partridge, *Polymer.*, **45**, 5868 (2005).
17. M.K. Um, D. Im, and B.S. Hwang, *Compos. Sci. Technol.*, **62**, 29 (2002).
18. S. Du, Z.S. Guo, B. Zhang, and Z. Wu, *Polym. Int.*, **53**, 1343 (2004).
19. J. Kratz, K. Hsiao, G. Fernlund, and P. Hubert, *J. Compos. Mater.*, **47**, 341 (2013).
20. L. Khoun, T. Centea, and P. Hubert, *J. Compos. Mater.*, **44**, 1397 (2010).
21. C.Y.M. Tung, and P.J.J. Dynes, *J. Appl. Polym. Sci.*, **27**, 569 (1982).
22. D. Kim, T. Centea, and S.R. Nutt, *Compos. Sci. Technol.*, **102**, 132 (2014).
23. P.J. Leider, *J. Ind. Eng. Chem. Fundam.*, **13**, 342 (1974).

Please cite the article as: D. Kim, and S.R. Nutt, “**Processability of DDS Isomers-Cured Epoxy Resin: Effects of Amine/Epoxy Ratio, Humidity, and Out-Time**” *Polymer Engineering and Science*. 2017. DOI: **10.1002/pen.24738**



24. P.J. Leider, and R.B. Bird, *Ind. Eng. Chem. Fundam.*, **13**, 336 (1974).